

University of Pretoria Department of Economics Working Paper Series

Predicting the Conditional Distribution of Risk Aversion The Role of Climate Risks in a Cross-Quantilogram Framework

Abeeb Olaniran
University of Pretoria
David Gabauer
Lincoln University
Rangan Gupta
University of Pretoria
Onur Polat
Bilecik Şeyh Edebali University
Working Paper: 2025-24
July 2025

Department of Economics University of Pretoria 0002, Pretoria South Africa Tel: +27 12 420 2413

Predicting the Conditional Distribution of Risk Aversion The Role of Climate Risks in a Cross-Quantilogram Framework

Abeeb Olaniran^a, David Gabauer^{b, *}, Rangan Gupta^a, and Onur Polat^c

^a Department of Economics, University of Pretoria, South Africa.
 ^b Department of Financial and Business Systems, Lincoln University, New Zealand.
 *Corresponding author: david.gabauer@lincoln.ac.nz
 ^c Department of Public Finance, Bilecik Seyh Edebali University, Turkey.

July 27, 2025

Abstract

Climate-related risks have become a growing source of market disruption, with potential behavioral implications for investor decision-making. This study investigates whether and how climate risks influence risk aversion among market participants. Using a quantilogram approach, we examine the predictive power of different climate risk measures, covering both physical and transition risks, for a behavioral proxy of investor risk aversion. The analysis yields three key findings. First, climate risks significantly increase risk aversion, particularly in the lower and median quantiles of climate risk and the upper quantiles of risk aversion. Second, physical risks exert a stronger influence than transition risks, with global warming and U.S. climate-related policy uncertainty emerging as the most impactful within their respective categories. Third, the observed effects remain robust after controlling for other sources of macroeconomic and financial uncertainty. These findings suggest that climate risks can dampen investor risk appetite, a result with important implications for financial market stability and the design of disaster-related financial policy interventions.

 $\underline{\text{Keywords: }} \ \underline{\text{Climate-related risks, Quantilogram frameworks, Quantiles, Predictability, }} \\ \underline{\text{Risk aversion.}}$

JEL codes: C21, C22, G32, G41, Q54.

1 Introduction

Risk-taking behavior is fundamental to the decision-making processes of various economic agents, including individuals and firms, who engage in such behavior with the expectation of earning returns greater than their initial stakes. In other words, the propensity to take financial risks is critical, as it is often a prerequisite for achieving higher returns (Fama and MacBeth, 1973; Campbell, 1996; Wang and Yang, 2013). Ideally, a range of factors is known to shape these risk preferences, including wealth (Cameron and Shah, 2015; Chao et al., 2017; Pool et al., 2019), background (Poletti-Hughes and Williams, 2019; Llanos-Contreras et al., 2021), experience (Shupp et al., 2017; Arslan et al., 2020; Guo et al., 2023), compensation mechanisms in the event of loss (Carpenter, 2000; Ross, 2004; Chaigneau, 2015), and governance (Llanos-Contreras et al., 2021).

Nevertheless, climate risk, among other sources of uncertainty, has increasingly been linked to the intensification of natural disasters, and consequently amplifying market fears in recent times (Johnson, 2010; Anderson and Robinson, 2019; Xiao and Liu, 2023). These fears often stem from various mitigation strategies, which include not only policy interventions but also regulatory requirements compelling firms to adopt safer and more environmentally sustainable business practices. As a result, climate-related concerns may influence investor commitment and confidence as well as alter the consumer consumption behavior (Daumas, 2021; Horn and Oehler, 2025; Liu and Yan, 2025), thereby exposing these agents to additional risks and shifting their risk preferences toward greater aversion.

Understanding how climate change influences risk appetite is crucial for assessing whether climate-related risks lead economic agents to shift away from risky assets toward safer alternatives. Examining the extent to which various climate risk measures affect this behavior provides insights into changing investor preferences. The implications of such shifts are significant for financial markets and the broader economy, as established in prior research. Elevated risk aversion, for example, may deter investors from seizing new opportunities or supporting innovative technologies. This behavioral shift can, in turn, reduce the effective-

ness of financial assistance packages following climate disasters, impede economic recovery, and suppress long-term growth (Bourdeau-Brien and Kryzanowski, 2020).

A deeper understanding of shifts in risk preferences requires a theoretical foundation that explains how natural disasters, particularly climate shocks, influence economic behavior. These events are increasingly viewed as rare disaster risks because of their potential to severely disrupt consumption, investment, production, and policy dynamics (Demirer et al., 2018). Such disruptions can alter the core drivers of investment behavior and heighten uncertainty, thereby diminishing the willingness of investors and managers to take risks (Bate, 2022).

This mechanism is well outlined in the real options theory advanced by Bernanke (1983), which posits that uncertainty (i.e., about climate-related risks) can heavily influence investment and consumption behavior, especially due to the substantial and often irreversible costs associated with sub-optimal decisions (see also, Salisu et al., 2023). Similarly, it is suggested that expectations about natural disasters influence individual behavior by altering perceptions of baseline risk. In essence, the occurrence of such events can serve as informational shocks that prompt individuals to revise their risk assessments, as those directly affected often find it difficult not to be impacted psychologically and are compelled to reassess their strategies (Cameron and Shah, 2015). Moreover, theoretical insights into utility maximization under background risk show that individuals tend to become more risk-averse when exposed to additional sources of uncertainty. As established by Gollier and Pratt (1996), the presence of background risk leads a utility-maximizing agent to prefer safer choices, a property known as risk vulnerability. This implies a greater demand for insurance or safer assets when individuals are confronted with external uncertainties. Thus, the channels identified by Bernanke (1983) and Gollier and Pratt (1996) provide a compelling theoretical rationale for why climate-related risks may increase risk aversion. Based on this premise, we hypothesize a positive relationship between climate-related risk and individual or investor risk aversion.

While several studies have sought to examine the relationship between natural disasters and risk preferences, their findings are often mixed, perhaps due to the use of survey-based measures of risk preferences, which tend to be subjective (see, Cameron and Shah, 2015; Shupp et al., 2017; Bourdeau-Brien and Kryzanowski, 2020; Hoang and Le, 2021; Ingwersen et al., 2023; Guo et al., 2023). To address this drawback, we contribute to the literature on disasters and shifting risk preferences by employing standard market-based measures of time-varying Risk Aversion index as developed by Bekaert et al. (2022), along with climate risk indicators from Faccini et al. (2023). Particularly, our contributions are in threefold as follows: (i) we go beyond the physical risks associated with natural disasters, commonly emphasized in the existing literature, by also considering transition risks stemming from policy strategies to address climate concerns, (ii) we further account for additional sources of risks, as outlined in the succeeding section, and conduct our empirical analysis within a quantilogram framework, and (iii) we utilize the cross-quantilogram, which allows us to study causal effects across different quantiles of Risk Aversion in response to varying sizes (and signs) of climate risks. Given the hypothesis that both physical and transition climate risks increase Risk Aversion, it is essential to test not only the causal direction but also the sign and magnitude of these effects. This frameworks is preferable over the causality-in-quantiles technique (see, for example, Jeong et al., 2012, in this regard), as it facilitates sign analysis and accommodates additional sources of risks as controls, via the partial cross-quantilogram (see, Han et al., 2016), and hence, can go beyond a bivariate analysis.

In essence, the cross-quantilogram approach enables us to explore directional relationships and nonlinear dependencies between climate risk and *Risk Aversion* across different points in their joint distributions. This is particularly valuable given the asymmetric and potentially tail-heavy nature of climate shocks, which may exert disproportionate influence on risk preferences in extreme situations. Unlike traditional mean- or median-based approaches common in studies that do not rely on survey data (e.g., Bourdeau-Brien and

Kryzanowski, 2020), the cross-quantilogram captures these heterogeneous effects more precisely, making it well-suited to our investigation.

Our empirical results reveal that climate risk has a generally positive and statistically significant effect on *Risk Aversion*, with these effects being more pronounced in the lower and median quantiles of climate risk, and in the upper quantiles of *Risk Aversion*, across multiple lags. Furthermore, given the number of statistically significant cross-quantilogram combinations across various lags, the physical risk component appears to have a greater impact than the transition risk component, with global warming and U.S. climate-related policy uncertainty contributing more in the respective categories. Importantly, the results remain robust even after controlling for other sources of risk.

The remainder of the paper is structured as follows. Section 2 introduces and describes the employed dataset. Section 3 outlines the empirical methodology while Section 4 interprets and discusses the obtained empirical results. Finally, Section 5 concludes the study.

2 Data

The datasets for the examination of the nexus between climate risk and risk aversion include the time-varying Risk Aversion index by Bekaert et al. (2022)¹, as well as the physical (global warming [GW] and natural disaster [ND]) and transition (climate-related international summits [IS] and U.S. climate-related policy uncertainty [USCP]) climate risk measures developed by Faccini et al. (2023)². The Risk Aversion index is constructed based on a utility-derived measure of risk aversion, capturing the representative agent's time-varying relative risk aversion. It incorporates six financial indicators: detrended earnings yield, corporate return spread, term spread (10-year minus 3-month), realized variance of equity returns, realized variance of corporate bond returns, and equity risk-neutral variance. These variables are combined using the Generalized Method of Moments (GMM), which estimates

¹Retrieved from https://www.nancyxu.net/risk-aversion-index

²Retrieved from https://docs.google.com/spreadsheets/d/14ewbq1JMgz0EJtog76Kti1fB39-P-pjk/edit?gid=614709312#gid=

their optimal linear combination under asset moment conditions aligned with a dynamic no-arbitrage asset pricing framework. The conditional variance linked to macroeconomic uncertainty is then projected onto these financial variables to generate the *Risk Aversion* index. Due to the limited availability of some macroeconomic uncertainty measures, such as industrial production at daily frequencies (available only monthly), the risk aversion index is produced at both daily and monthly frequencies. However, this study relies on the daily version of the index.

On the other hand, the development of physical and transition risk indices utilizes the Latent Dirichlet Allocation (LDA) method to identify and differentiate climate-related risk factors. This approach involves extracting textual data related to four climate-focused themes: natural disasters, global warming, U.S. climate policy, and international climate-change summits from over thirty-four thousand articles published in Thomson Reuters News Archive between January 2000 and December 2018. These topics are grouped into two categories: physical risks (comprising climate-related natural disasters and global warming) and transition risks (including U.S. climate-related policy and climate-related international summits). The textual data includes terms like "weather," "drought," "flood," and "storm" for natural disasters; "temperature," "heat," "greenhouse," "emission," and "Celsius" for global warming; "Kyoto," "protocol," "summit," and "Copenhagen" for international summits; and "Clinton," "environmental," "congress," and "campaign" for U.S. climate policy.

In addition, the information content of many other uncertainty indicators, including equity market volatility index (EMV-ID) (Baker et al., 2020)³, geopolitical risk index (GPR) (Caldara and Iacoviello, 2022)⁴, supply bottleneck index (SBI)⁵ (Burriel et al., 2024), and trade policy uncertainty (TPU)⁶, is obtained via the principal component analysis frame-

³Retrieved from https://www.policyuncertainty.com/infectious_EMV.html

⁴Retrieved from https://www.matteoiacoviello.com/gpr.htm

⁵https://www.bde.es/wbe/en/areas-actuacion/analisis-e-investigacion/recursos/indices-de-cuellos-de-botella-en-la-oferta-basados-en-articulos-de-prensa.html. To have the aggregate from the seven economies available, we calculate the average based on the available data for each period. For instance, if the index is available for only two countries during a given period, the average is computed across those two countries rather than the entire seven.

⁶Retrieved from https://policyuncertainty.com/trade_uncertainty.html

work, and this is thereafter incorporated as an additional control variable in our formal analysis. The inclusion of these variables as controls is motivated by their roles in capturing various dimensions of disaster-related risks. Each of these indices reflects different types of uncertainty or shocks that can significantly influence economic behavior and investor sentiment. For instance, the EMV-ID captures broad financial market uncertainty, often linked to macroeconomic shocks; the GPR index measures geopolitical tensions that may escalate into global crises; the SBI captures disruptions in supply chains, which can have widespread economic implications; and the TPU reflects uncertainty surrounding trade policy, which can affect global trade flows and investment decisions. Given that these variables represent systemic risks or potential disaster channels, it is important to control for them to isolate the specific effects of the variables of interest in our analysis.

A comparison of the statistical properties of our risk aversion measures, as presented in Table 1, shows that the measure proposed by Bekaert et al. (2022) is higher, on average, than the one derived from the other uncertainty measures via PCA. For the climate risk measures, the transition risk measures - 0.613 for IS and 0.712 for USCP - are consistently higher than the physical risk measures, which stand at 0.566 for GW and 0.584 for ND.

[INSERT TABLE 1 AROUND HERE.]

All the series, including the *Risk Aversion* and climate risk measure, are positively skewed, while the kurtosis statistics indicate leptokurtic distributions (as the kurtosis values are in excess of 3), suggesting heavy tails in the data. This departure from normality is further confirmed by the rejection of the normality assumption, as indicated by the statistical significance of the Jarque-Bera test results.

In addition to these statistical features, we examine the potential co-movements between our measure of *Risk Aversion* and both physical and transition climate risks. We observe a positive co-movement between each of the climate risk proxies and *Risk Aversion*, particularly during the 2008/2009 and 2019/2020 periods, suggesting that climate risks may increase risk intolerance among investors and other economic agents (see Figures 1 and 2).

Nonetheless, this observation alone is insufficient for reliable conclusions. Hence, additional empirical analyses are conducted for validity.

[INSERT FIGURES 1 AND 2 AROUND HERE.]

Given the distributional property of our series and to justify our choice of empirical technique, we conducted several pre-estimation tests, including the Granger causality test, stability test, and the BDS test.

The Granger causality test (Granger, 1969), which examines the null hypothesis that climate risk does not Granger-cause *Risk Aversion*, is presented in Table 2. The results show that the null hypothesis of no causality between climate risk and *Risk Aversion*, particularly for the physical risk measures, cannot be rejected. This indicates that only the transition risk Granger-causes *Risk Aversion*, albeit weakly.

[INSERT TABLE 2 AROUND HERE.]

Furthermore, we test for possible misspecification in the model. This is achieved by recovering the residual of the associated risk aversion—climate risk model, and performing a linearity test using the BDS test. The results, where we find overarching evidence of non-linearity, given the rejection of the null hypothesis that the model is independently and identically distributed, are presented in Table 3.

[INSERT TABLE 3 AROUND HERE.]

Similarly, we test whether the non-causality above could be traced to plausible structural breaks. Therefore, we use Bai and Perron (2003) global test for multiple structural breaks (UDMax statistic) for this purpose. The results indicate the presence of structural break(s) or parameter instability at multiple dates (most notably during the global financial crisis of 2008, the oil price crash of 2016, and the declaration of COVID-19 as a global pandemic in March 2020) as well as across several climate risk variables (see Table 4). This instability may explain why climate risk does not strongly Granger-cause risk aversion.

[INSERT TABLE 4 AROUND HERE.]

In addition, we present the quantile causality results (see, Jeong et al., 2012) for both physical and transition climate-related risks using the time-varying *Risk Aversion* measure⁷. The traditional Granger causality test shows no evidence of causality. Table 5 reveals strong evidence that climate risk generally causes changes in *Risk Aversion* across various quantiles, suggesting that rising climate-related risks influence economic agents by increasing their tendency to become more risk-averse.

[INSERT TABLE 5 AROUND HERE.]

Given these pre-tests, we employ the cross-quantilogram framework to explore the relationship between climate risk and *Risk Aversion* in the succeeding section. This framework is suitable as it enables us to examine both the direction and magnitude of climate risk impacts on *Risk Aversion* in the short- and long-run, based on multiple lag structures. In addition, the framework allows us to control for other predictors through the use of the cross-partial quantilogram.

3 Methodology

To investigate directional predictability and dependence between climate-related risks and Risk Aversion across various distributional regions, we employ the cross-quantilogram framework⁸ introduced by Han et al. (2016). This methodology enables the identification of quantile-specific and lag-dependent relationships that are not captured by traditional linear correlation or Granger causality approaches.

⁷Beyond this measure, we also employ an alternative *Risk Aversion* measure representing an aggregated index of global risk-on/risk-off (RoRo) states developed by Chari et al. (2023) (https://anushachari.weebly.com/roro.html). This index captures variation across four broad categories: advanced economy credit risk (RoRo CR), equity market volatility (RoRo Equity), funding conditions (RoRo Liquidity), and currencies and gold (RoRo CurrGold). Using this measure to test for causality yields consistent results as *Risk Aversion* (see Table A.1 in the appendix).

⁸Beyond this bivariate analysis, we account for additional variables that may influence the nexus between climate risk and *Risk Aversion*. To this end, the partial cross-quantilogram framework is employed, with the associated methodological framework and corresponding results provided in the appendix. Essentially, the results are quantitatively similar to cross-quantilogram.

Thus, we assume $\{Y_t\}_{t=1}^T$ and $\{X_t\}_{t=1}^T$ (that is, *Risk Aversion* and of climate risk, respectively) denote two stationary time series. Also, for a specific quantile levels $\tau_1, \tau_2 \in (0,1)$, we take $q_Y(\tau_1)$ and $q_X(\tau_2)$ to denote the marginal τ_1 - and τ_2 -quantiles of Y_t and X_t , respectively. we then define the quantile-hit process as:

$$\psi_t^Y(\tau_1) = \mathbf{1}\{Y_t \le q_Y(\tau_1)\} - \tau_1,\tag{1}$$

$$\psi_t^X(\tau_2) = \mathbf{1}\{X_t \le q_X(\tau_2)\} - \tau_2,\tag{2}$$

where $\mathbf{1}\{\cdot\}$ is the indicator function. These quantile-hit processes are mean-zero and capture deviations from the unconditional quantile expectations.

The cross-quantilogram at lag $k \in \mathbb{Z}_+$ is defined as the correlation between the lagged quantile-hit process of X_t (i.e., climate risk measures) and the contemporaneous quantile-hit process of Y_t (i.e., the dependent variable - $Risk\ Aversion$):

$$\rho_{\tau_1,\tau_2}(k) = \frac{\mathbb{E}[\psi_t^Y(\tau_1) \cdot \psi_{t-k}^X(\tau_2)]}{\sqrt{\mathbb{E}[\psi_t^Y(\tau_1)^2] \cdot \mathbb{E}[\psi_{t-k}^X(\tau_2)^2]}}.$$
(3)

This measure captures the directional quantile dependence from X_{t-k} to Y_t . A significant nonzero value of $\rho_{\tau_1,\tau_2}(k)$ indicates that realizations of X at lag k within the τ_2 -quantile region are predictive of the occurrence of values in the τ_1 -quantile region of Y.

In practice, the cross-quantilogram is estimated as:

$$\hat{\rho}_{\tau_1,\tau_2}(k) = \frac{\sum_{t=k+1}^T \hat{\psi}_t^Y(\tau_1) \cdot \hat{\psi}_{t-k}^X(\tau_2)}{\sqrt{\sum_{t=k+1}^T \hat{\psi}_t^Y(\tau_1)^2} \cdot \sqrt{\sum_{t=k+1}^T \hat{\psi}_{t-k}^X(\tau_2)^2}},\tag{4}$$

where the quantiles $q_Y(\tau_1)$ and $q_X(\tau_2)$ are estimated using the empirical distribution functions of Y_t and X_t , respectively.

To test for the absence of directional predictability across multiple lags, we use a Box-Ljung-type statistic defined as:

$$\hat{Q}_{\tau_1,\tau_2}^{(p)} = T \sum_{k=1}^{p} \hat{\rho}_{\tau_1,\tau_2}(k)^2, \tag{5}$$

where p denotes the maximum lag under consideration. Under the null hypothesis of no directional predictability from climate risk (X) to $Risk\ Aversion\ (Y)$ at the specified quantiles and lags, the test statistic $\hat{Q}_{\tau_1,\tau_2}^{(p)}$ follows a nonstandard distribution. Consequently, critical values are obtained via $stationary\ bootstrap$ procedures or self-normalized inference to ensure valid size control.

This approach allows for the detection of asymmetric and nonlinear dependence structures, including tail dependence and regime-specific spillovers, which are particularly relevant in financial and macroeconomic contexts.

4 Empirical Results

The cross-quantilogram, unlike the quantilogram developed by Linton and Whang (2007)⁹, is employed to assess the dependence between climate risks and *Risk Aversion*, as well as to evaluate the direction of predictability between these two key variables. This method is particularly appealing given its ability to capture co-movements in the tails of distributions, making it well-suited for analyzing extreme events. Particularly, the cross-quantilogram facilitates the examination of quantile-to-quantile associations between two distinct time series. Another attraction to this approach lies in its capacity to accommodate a more extensive lag structure, which contrasts with the limitations of conventional quantile regression methods that typically restrict the number of lags.

This section is partitioned into two parts: Section 4.1 presents the results of the cross-quantilogram analysis between climate risks and *Risk Aversion*, while Section 4.2 focuses on the portmanteau test (Q-statistics) for evaluating their joint dynamics or significance. To have a broader view on how uncertainty influences *Risk Aversion*, we also extend the analysis by incorporating economic-wide risk indicators (as outlined in Section 2) using a partial cross-quantilogram framework. Nonetheless, in order not to deviate from the main focus of the impact of climate risks on *Risk Aversion*, these supplementary results are

⁹This is the univariate form of the quantilogram method, which assesses predictability across various segments of a stationary distribution (of a variable) by analyzing the correlogram of quantile hits

reported in the appendix.

4.1 Cross-quantilogram between climate risk and Risk Aversion

As previously mentioned, this subsection presents the results on the predictability of climate risks, specifically, physical risks (GW and ND) and transition risks (IS and USCP), for *Risk Aversion*. We show the cross-quantilogram plots across quantiles that capture the predictive relationship from climate risks to *Risk Aversion* over various lags (1–60), along with the associated 95% bootstrapped confidence intervals. Specifically, we partition the distribution of *Risk Aversion* into deciles ranging from 0.1 to 0.9, while climate risk is represented by three key quantiles: 0.1, 0.5, and 0.9. These quantiles correspond to the lower tail (0.1–0.4 for *Risk Aversion* and 0.1 for climate risk), the median (0.5 for both), and the upper tail (0.6–0.9 for *Risk Aversion* and 0.9 for climate risk) of their respective distributions. These results are illustrated in Figures 3 to 6, corresponding to GW, ND, IS, and USCP, respectively.

In Figure 3, the cross-quantilograms at the lower quantiles of $Risk\ Aversion$ are generally positive but statistically insignificant across most lags, except for a few instances at quantiles 0.3 and 0.4, particularly at the later lag (of 60) corresponding to the lower and middle tails of GW. In contrast, we observe significantly positive relationships across multiple (or nearly all) lags for the higher quantiles of $Risk\ Aversion\ (0.6\ to\ 0.9)$ and for the 0.1 and 0.5 quantiles of GW. Notwithstanding the positive relationship at the upper quantile of $GW\ (0.9)$, the observed association is mostly not statistically significant. These findings suggest that GW exerts a predictive influence on $Risk\ Aversion\$ primarily when it is at its lower and median levels (i.e., the lower and middle quantiles). However, this predictive relationship becomes more evident only at the upper quantiles of $Risk\ Aversion\$, indicating heightened sensitivity among investors and economic agents during periods of elevated market fear orchestrated by climate risk. By implication, when global warming indicators are relatively low or stable, they may still serve as early signals for rising risk aversion, particularly among those already positioned at the higher end of the risk-averse spectrum.

[INSERT FIGURE 3 AROUND HERE.]

Figure 4 illustrates the cross-quantilogram estimates from ND to $Risk\ Aversion$. The result is in sharp contrast to the pattern observed for GW. The dependence is more prevalent at the lower quantiles of $Risk\ Aversion$, particularly when paired with the lower and middle quantiles of ND, with the positive relationship becoming more significant at longer lags (save for the combination (0.2 and 0.5)), which shows significance across the entire lag structure). Moreover, at the median and upper quantiles of $Risk\ Aversion\ (0.5\ to\ 0.9)$ combined with the lower and middle quantiles of $ND\ (0.1\ and\ 0.5)$, the relationship also covers the entire lag structure.

Put differently, unlike GW, ND shows significant positive dependence with the lower and upper quantiles of Risk Aversion. Notably, most quantile combinations between ND and Risk Aversion are statistically significant at the 5% level, except for combinations involving the highest ND (0.9).

Overall, climate-related natural disasters appear to play a more important role in predicting the $Risk\ Aversion$ tendencies of investors and other economic agents, as evidenced by the greater number of significant cross-quantilogram combinations observed. Nonetheless, it is important not to overlook the mild or moderate GW signals, as these can trigger amplified risk responses, particularly among more cautious market participants or during already periods of elevated climate-related uncertainty.

[INSERT FIGURE 4 AROUND HERE.]

Turning to transition risk, Figure 5 reports the cross-quantilogram estimates from *IS* to *Risk Aversion*. The results reveal no clear dependence pattern, though some quantile combinations exhibit statistically significant relationships, particularly at longer lags. The significant associations primarily occur at the median quantile of *Risk Aversion*, while both the lower and upper tails show limited or no dependence. This suggests a modest role of *IS* in influencing risk perception under normal market conditions.

[INSERT FIGURE 5 AROUND HERE.]

A contrasting picture emerges for *USCP*, as shown in Figure 6. Here, statistically significant dependence is observed across virtually all quantile combinations at several lags. These results underline the critical importance of *USCP* in shaping *Risk Aversion*, reflecting its pervasive influence across the entire risk spectrum.

The stronger influence of *USCP* on *Risk Aversion*, compared to *international climate-related summits (IS)*, may be attributed to the uncertainty surrounding the U.S. government's decision to withdraw from the Paris Agreement. Investors could interpret this move as a negative signal, especially in light of the pro-emission-reduction policies pursued by other developed nations, and may delay investment commitments due to concerns about potential reciprocal actions from international climate organizations and other environmentally focused entities. Interestingly, *IS* appears to have a weaker impact on *Risk Aversion*, which may reflect investors and other economic agents' confidence in ongoing global mitigation efforts.

[INSERT FIGURE 6 AROUND HERE.]

When comparing the effects of physical and transition climate risks, the findings suggest that physical risks exert a stronger influence on *Risk Aversion*, as indicated by a greater number of significant cross-quantilogram combinations observed¹⁰. This again underscores the trust investors place in mitigation strategies aimed at managing transition-related risks, which are easier to manage than the physical-related climate events, which tend to be unpredictable.

Given our hypothesis of a positive relationship between climate-related risk and *Risk* Aversion which is grounded in both real options theory and risk vulnerability theory, we find support for our findings in related studies, including research on the impact of both natural and man-made disasters on individuals' risk preferences (e.g., Cameron and Shah,

¹⁰These results remain consistent even after accounting for other measures of risk (See Figures A.1 to A.4 in the Appendix).

2015; Shupp et al., 2017; Bourdeau-Brien and Kryzanowski, 2020; Hoang and Le, 2021; Guo et al., 2023; Ingwersen et al., 2023). For instance, Shupp et al. (2017) show that individuals affected by tornadoes became more risk-averse, with those who lost a friend or neighbor also exhibiting increased loss aversion. Similarly, Hoang and Le (2021) provide evidence that asset loss from natural disasters leads households to adopt more risk-averse behaviors. Conversely, Ingwersen et al. (2023) find that individuals directly exposed to a tsunami displayed temporarily higher risk tolerance compared to those not directly affected, as survivors were more willing to take financial risks during the post-disaster recovery period. This short-term shift in risk-taking behavior aligns with the findings of (Bourdeau-Brien and Kryzanowski, 2020), who also observe a temporary increase in risk appetite following disaster events.

4.2 Box-Ljung Q statistics between climate risk and Risk Aversion

We present the corresponding portmanteau tests, which assess the joint dynamics and overall significance of the cross-quantilogram-based predictability results of climate risks for $Risk\ Aversion$. These tests employ the Box-Ljung Q statistics across various lag orders and distinct quantile combinations. As shown in Figures 7 to 10, the results confirm the significant lag structures previously identified in the cross-quantilograms.

Specifically, Figure 7 indicates that the Box-Ljung test statistics are largely significant for $Risk\ Aversion$, especially from the lower quantiles (around 0.4, except when paired with GW at 0.5) through the median and upper quantiles (0.5 to 0.9), when combined with the lower and middle quantiles of GW, and consistently across the entire lag structure.

[INSERT FIGURE 7 AROUND HERE.]

Similarly, the portmanteau test for ND and Risk Aversion mirrors what is observed in Figure 4, with a notable distinction from GW in Figure 7. In the case of ND, there is evidence of mixed significance across both the short and long lags (see Figure 8). For example, at the lower quantile of ND (corresponding to the first column of Figure 8), the

influence of ND on $Risk\ Aversion$ is significant across all quantiles of ND and throughout the entire lag structure. In contrast, at the middle quantile of ND (corresponding to the middle column of Figure 8), the significance is largely mixed along the short and long lags. Nonetheless, it is only in the quantile combination (($\tau_1 = 0.1$ and ($\tau_2 = 0.9$) we have a significant relationship from lag 10 onwards.

[INSERT FIGURE 8 AROUND HERE.]

Furthermore, Figures 9 and 10 for the portmanteau tests of *IS* and *USCP* also reinforce the results of the significant relationships previously obtained in Figures 5 and 6, respectively.

[INSERT FIGURES 9 AND 10 AROUND HERE.]

5 Concluding Remarks

This study examines the predictability of climate risks for *Risk Aversion* (Bekaert et al., 2022), with a focus on the distinct roles played by different measures of climate risk. It also seeks to determine whether physical or transition climate risks have a greater impact on *Risk Aversion*. While considerable efforts have been made to examine the predictive power of natural disasters for risk preferences, the role of the climate-related risks, particularly transition risk, remains under-researched.

The nexus between climate-related risks and risk aversion is grounded in two theoretical underpinnings, including Bernanke (1983) and Gollier and Pratt (1996), which suggest that natural disasters can significantly influence individual and investor risk preferences. While the main focus is on the link between climate risks and Risk Aversion, the study also considers additional variables that may affect this relationship. Accordingly, other sources of risk are incorporated into our quantilogram framework (Han et al., 2016), and as such, we explore the causal effects across different quantiles of Risk Aversion in response to varying magnitudes and directions (positive or negative) of climate risk shocks. By comparing the effects of physical and transition risks, this study addresses a timely and relevant research

question concerning the predictive power of climate-related events, which have been largely under-researched. In doing so, it provides valuable insights into the role these events play in shaping risk-taking behavior.

Our findings indicate that climate risks have a generally positive and statistically significant effect on Risk Aversion, particularly at the lower and median quantiles of climate risk and the upper quantiles of Risk Aversion, across various lags. These results support the formulated hypothesis of a positive relationship between climate-related risks and Risk Aversion. Notably, the physical risk component appears to exert a greater influence than the transition risk component. Within the physical risk category, global warming has a stronger impact on Risk Aversion, while among transition risks, U.S. climate-related policy uncertainty exerts a stronger effect than international climate-related summits.

These findings carry important implications for policymakers seeking to design effective mitigation strategies to address climate risks. Specifically, strategies developed when investor sentiment is characterized by heightened risk aversion are less likely to achieve their intended goals. Therefore, policymakers must consider incentive-based and confidence-building measures – such as consistent and credible policies – to encourage greater risk tolerance for the broader benefit of the economy.

Given the study's focus on climate risk measures and general investor behavior, future research could build on this analysis by incorporating behavioral factors such as investor sentiment to better understand how perceptions of climate risk influence risk-taking decisions. Furthermore, examining the role of regulatory responses and adaptation strategies may also shed light on how policy moderates these effects. Cross-country analyses, particularly between developed and emerging economies, could further uncover contextual differences in climate risk sensitivity that this study does not account for.

References

- Anderson, A. and Robinson, D. T. (2019). Climate fears and the demand for green investment. Swedish House of Finance Research Paper, 1(19-14).
- Arslan, R. C., Brümmer, M., Dohmen, T., Drewelies, J., Hertwig, R., and Wagner, G. G. (2020). How people know their risk preference. *Scientific Reports*, 10(1):15365.
- Bai, J. and Perron, P. (2003). Critical values for multiple structural change tests. *The Econometrics Journal*, 6(1):72–78.
- Baker, S. R., Bloom, N., Davis, S. J., Kost, K., Sammon, M., and Viratyosin, T. (2020). The unprecedented stock market reaction to COVID-19. *The Review of Asset Pricing Studies*, 10(4):742–758.
- Bate, A. F. (2022). The nexus between uncertainty avoidance culture and risk-taking behaviour in entrepreneurial firms' decision making. *Journal of Intercultural Management*, 14(1):104–132.
- Bekaert, G., Engstrom, E. C., and Xu, N. R. (2022). The time variation in risk appetite and uncertainty. *Management Science*, 68(6):3975–4004.
- Bernanke, B. S. (1983). Irreversibility, uncertainty, and cyclical investment. *The Quarterly Journal of Economics*, 98(1):85–106.
- Bourdeau-Brien, M. and Kryzanowski, L. (2020). Natural disasters and risk aversion. *Journal of Economic Behavior and Organization*, 177:818–835.
- Burriel, P., Kataryniuk, I., Pérez, C. M., and Viani, F. (2024). A new supply bottlenecks index based on newspaper data. *International Journal of Central Banking*, 20(2):17–67.
- Caldara, D. and Iacoviello, M. (2022). Measuring geopolitical risk. *American Economic Review*, 112(4):1194–1225.
- Cameron, L. and Shah, M. (2015). Risk-taking behavior in the wake of natural disasters. Journal of Human Resources, 50(2):484–515.
- Campbell, J. Y. (1996). Understanding risk and return. *Journal of Political Economy*, 104(2):298–345.
- Carpenter, J. N. (2000). Does option compensation increase managerial risk appetite? The Journal of Finance, 55(5):2311–2331.
- Chaigneau, P. (2015). Risk aversion, prudence, and compensation. *The European Journal of Finance*, 21(15):1357–1373.
- Chao, H., Ho, C.-Y., and Qin, X. (2017). Risk taking after absolute and relative wealth changes: The role of reference point adaptation. *Journal of Risk and Uncertainty*, 54(2):157–186.
- Chari, A., Stedman, K. D., and Lundblad, C. (2023). Risk-on risk-off: A multifaceted approach to measuring global investor risk aversion. Technical report, National Bureau of Economic Research.
- Daumas, L. (2021). Should we fear transition risks A review of the applied literature. FAERE-French Association of Environmental and Resource Economists Working Papers, 1(2021.05).
- Demirer, R., Gupta, R., Suleman, T., and Wohar, M. E. (2018). Time-varying rare disaster risks, oil returns and volatility. *Energy Economics*, 75:239–248.
- Faccini, R., Matin, R., and Skiadopoulos, G. (2023). Dissecting climate risks: Are they reflected in stock prices? *Journal of Banking and Finance*, 155:106948.
- Fama, E. F. and MacBeth, J. D. (1973). Risk, return, and equilibrium: Empirical tests. Journal of Political Economy, 81(3):607–636.

- Gollier, C. and Pratt, J. W. (1996). Risk vulnerability and the tempering effect of background risk. *Econometrica*, pages 1109–1123.
- Granger, C. W. (1969). Investigating causal relations by econometric models and cross-spectral methods. *Econometrica*, pages 424–438.
- Guo, L., He, W., and Wang, J. (2023). Disaster experience and resident risk preference: Evidence from China household finance survey. *PLoS One*, 18(11):e0295146.
- Han, H., Linton, O., Oka, T., and Whang, Y.-J. (2016). The cross-quantilogram: Measuring quantile dependence and testing directional predictability between time series. *Journal of Econometrics*, 193(1):251–270.
- Hoang, T. X. and Le, N. V. (2021). Natural disasters and risk aversion: Evidence from Vietnam. In *Natural Resources Forum*, volume 45, pages 211–229. Wiley Online Library.
- Horn, M. and Oehler, A. (2025). Attention, ESG, and Retail Investor Stock Holdings. *Journal of Behavioral Finance*, pages 1–19.
- Ingwersen, N., Frankenberg, E., and Thomas, D. (2023). Evolution of risk aversion over five years after a major natural disaster. *Journal of Development Economics*, 163:103095.
- Jeong, K., Härdle, W. K., and Song, S. (2012). A consistent nonparametric test for causality in quantile. *Econometric Theory*, 28(4):861–887.
- Johnson, L. (2010). Climate change and the risk industry: The multiplication of fear and value. In *Global Political Ecology*, pages 199–216. Routledge.
- Linton, O. and Whang, Y.-J. (2007). The quantilogram: With an application to evaluating directional predictability. *Journal of Econometrics*, 14(1):2250–282.
- Liu, Y. and Yan, B. (2025). Correlation between investor sentiment and carbon price considering economic policy uncertainty. *Journal of Behavioral Finance*, 26(1):64–81.
- Llanos-Contreras, O., Arias, J., and Maquieira, C. (2021). Risk taking behavior in Chilean listed family firms: A socioemotional wealth approach. *International Entrepreneurship and Management Journal*, 17(1):165–184.
- Poletti-Hughes, J. and Williams, J. (2019). The effect of family control on value and risk-taking in Mexico: A socioemotional wealth approach. *International Review of Financial Analysis*, 63:369–381.
- Pool, V. K., Stoffman, N., Yonker, S. E., and Zhang, H. (2019). Do shocks to personal wealth affect risk-taking in delegated portfolios? *The Review of Financial Studies*, 32(4):1457–1493.
- Ross, S. A. (2004). Compensation, incentives, and the duality of risk aversion and riskiness. *The Journal of Finance*, 59(1):207–225.
- Salisu, A. A., Gupta, R., and Olaniran, A. (2023). The effect of oil uncertainty shock on real GDP of 33 countries: A global VAR approach. *Applied Economics Letters*, 30(3):269–274.
- Shupp, R., Loveridge, S., Skidmore, M., Lim, J., and Rogers, C. (2017). Risk, loss, and ambiguity aversion after a natural disaster. *Economics of Disasters and Climate Change*, 1(2):121–142.
- Wang, J. and Yang, M. (2013). On the risk return relationship. *Journal of Empirical Finance*, 21:132–141.
- Xiao, J. and Liu, H. (2023). The time-varying impact of uncertainty on oil market fear: Does climate policy uncertainty matter? *Resources Policy*, 82:103533.

Table 1: Summary statistics

	Mean	Median	Max.	Min.	Std. Dev.	Skew	Kurt	J-B	Obs.
Risk Aversion	3.094	2.804	32.711	2.425	1.393	10.853	169.241	6143769.00***	5246
PC	0.000	-0.660	10.429	-1.192	1.486	2.292	8.724	11753.81***	5246
GW	0.566	0.379	6.170	0.000	0.633	2.420	12.298	24018.61***	5246
ND	0.584	0.278	9.003	0.000	0.869	3.193	17.157	52724.97***	5246
IS	0.613	0.248	17.690	0.000	1.077	4.754	41.776	348415.30***	5246
USCP	0.712	0.431	7.962	0.000	0.856	2.320	10.791	17977.06***	5246

Note: Risk Aversion refers to the time-varying risk aversion index developed by Bekaert et al. (2022). PC represents the filtered risk aversion index constructed through principal component analysis (PCA) using several uncertainty indicators, including the Equity Market Volatility Index (EMV-ID), Geopolitical Risk Index (GPR), Supply Bottleneck Index (SBI), and Trade Policy Uncertainty (TPU). GW, ND, IS, and USCP denote global warming, natural disasters (physical risk), climate-related international summits, and U.S. climate-related policy uncertainty (transition risk), respectively. Max., Min., Std. Dev., Skew, Kurt, J-B, and Obs. denote maximum, minimum, standard deviation, skewness, kurtosis, Jarque-Bera, and number of observations, respectively.

Table 2: Granger causality tests

	GW	ND	IS	USCP
Risk Aversion	1.3395	0.3357	1.8261*	2.4258**

Note: Both the dependent (Risk Aversion) and independent (climate risk) variables are stationary at level [i.e., I(0)] and the maximum lag length as suggested by the Schwarz information criterion is 5. ** and * indicate significance at the 5% and 10% levels, respectively. Null hypothesis: Climate risk does not cause Risk Aversion.

Table 3: BDS linearity tests

Dimension	GW	ND	IS	USCP
2	45.0492***	43.5483***	41.9437***	41.9085***
3	51.8936***	50.4534***	48.8041***	48.7658***
4	56.6489***	55.1880***	53.6405***	53.4410***
5	61.5222***	60.2462***	58.5981***	58.6955***
6	67.2139***	66.3064***	64.4678***	64.7163***
Included observations	5246	5246	5246	5246

Note: *** indicates significance at the 1% level. Null hypothesis (H₀): The variables are independently and identically distributed.

Table 4: Stability tests

Physical Risk									
	Global W	Varming	Natural Disaster						
	No. of breaks	Break dates	No. of breaks	Break dates					
Risk Aversion	3	$\begin{array}{c} 10/21/2008 \\ 11/25/2016 \\ 03/17/2020 \end{array}$	3	$\begin{array}{c} 10/21/2008 \\ 11/22/2016 \\ 03/17/2020 \end{array}$					
Observations (less the lag): 5241									
	Transition Risk								
	Internationa	al Summits	U.S. Clima	te Policy					
	No. of breaks	Break dates	No. of breaks	Break dates					
Risk Aversion	3	10/21/2008 11/25/2016 03/17/2020	3	10/21/2008 11/10/2016 03/17/2020					
Observations (less the lag): 5241									

Note: We apply the Bai-Perron multiple breakpoint test with the 'global L-breaks vs. none' (using UDMax determined breaks) option and allow for differing error distributions across regimes (Bai and Perron, 2003).

Table 5: Quantile causality between climate risks and Risk Aversion

Quantiles	0.1	0.2	0.3	0.4	0.5	0.6	0.7	0.8	0.9
GW to Risk Aversion	21.296***	21.144***	21.213***	17.640***	13.531***	10.501***	8.988***	9.995***	9.001***
ND to Risk Aversion	25.911***	23.588***	22.824***	17.658***	11.756^{***}	8.213***	6.999***	9.266***	10.515***
IS to Risk Aversion	30.791***	28.407^{***}	26.983***	19.352***	12.016***	7.804***	6.621^{***}	8.031***	8.765***
USCP to Risk Aversion	24.115^{***}	24.691^{***}	23.239***	18.644***	13.754***	9.259^{***}	7.845^{***}	9.067^{***}	9.529^{***}

Note: *** indicates significance at the 1% level. Null hypothesis (H₀): There is no causality between climate risks and Risk Aversion.

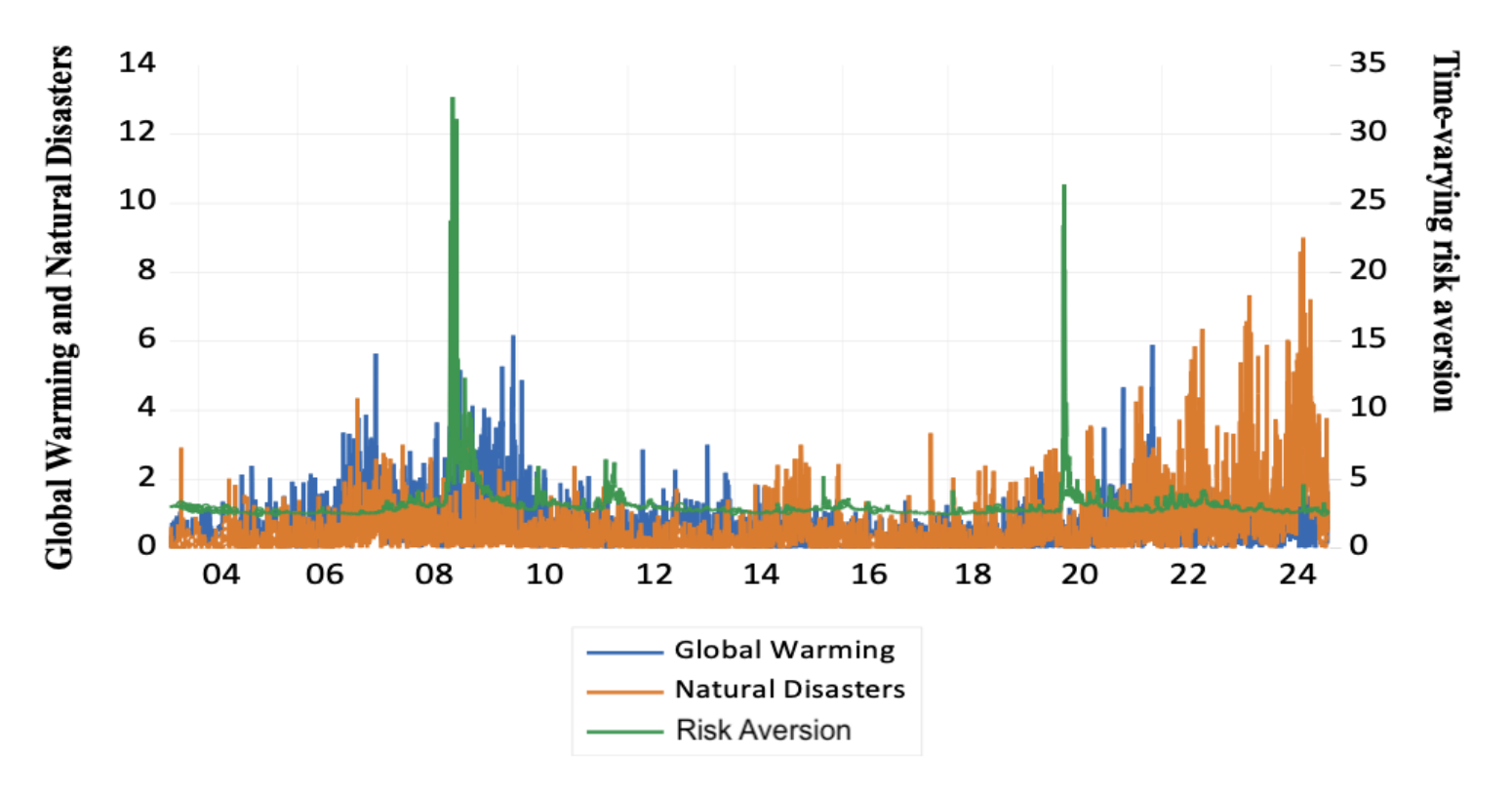


Figure 1: Co-movement between physical climate risk and Risk Aversion

Note: The measures of physical climate risk (global warming and natural disasters) occupy the left axis, while Risk

Aversion (Bekaert et al., 2022) is on the right axis.

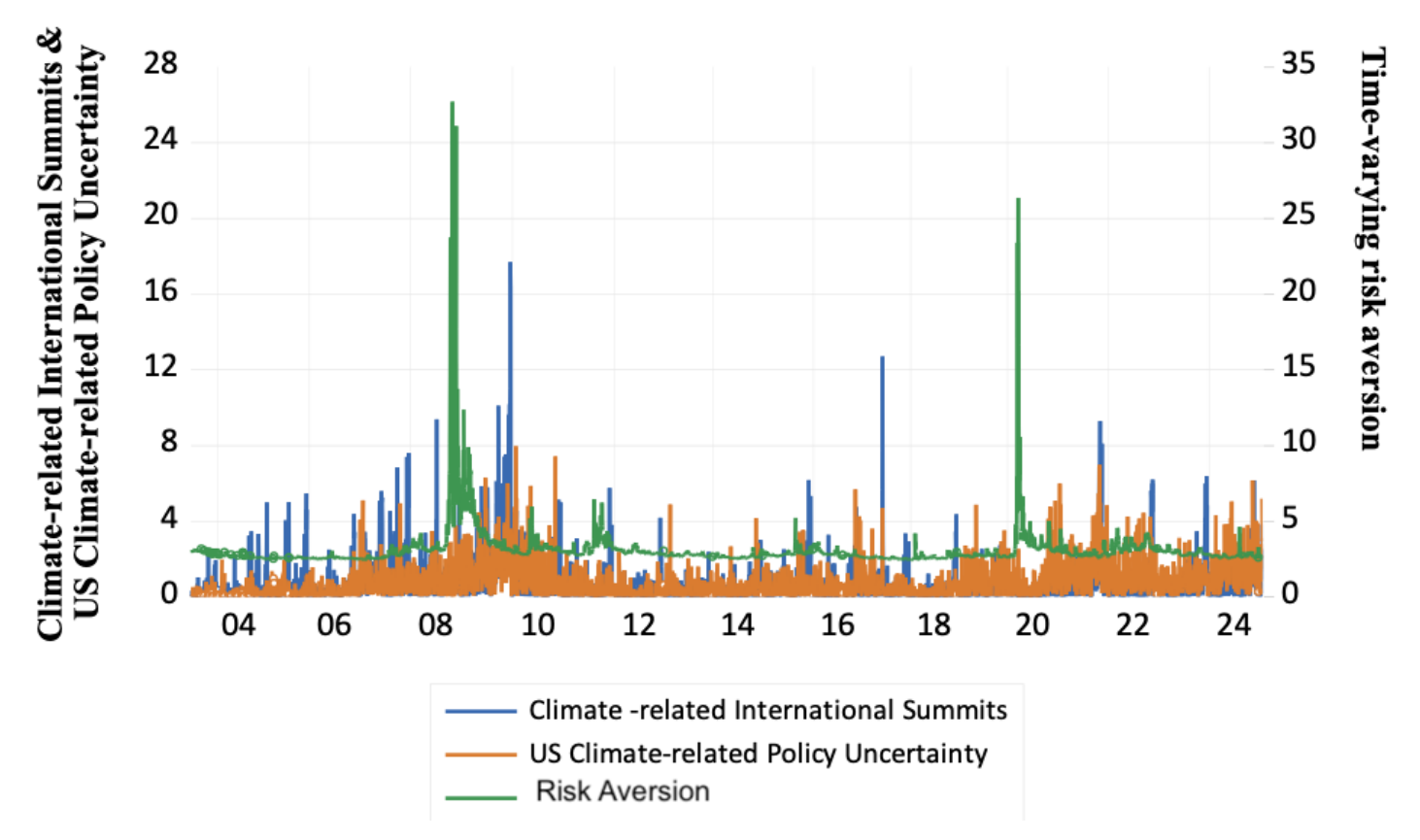


Figure 2: Co-movement between transition climate risk and Risk Aversion

Note: The measures of transition climate risk (climate-related international summits and U.S. climate-related policy uncertainty) occupy the left axis, while Risk Aversion (Bekaert et al., 2022) is on the right axis.

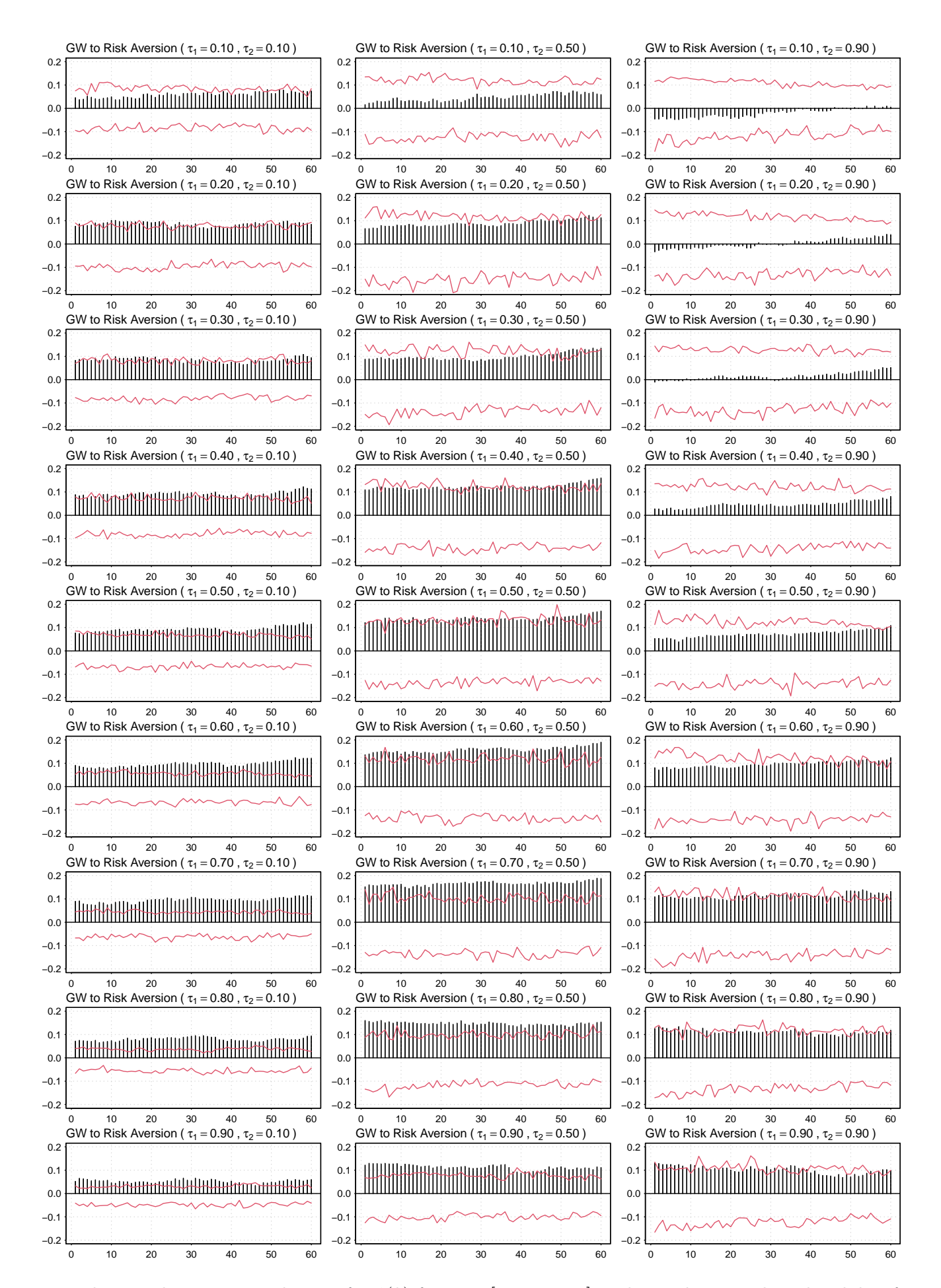


Figure 3: The sample cross-quantilogram for $\hat{\rho}(k)$ for $\tau_2 = [0.1, 0.5, 0.9]$ to detect directional predictability from GW to Risk Aversion. Bar graphs describe sample cross-quantilograms and lines are the 95% bootstrap confidence intervals centered at zero.

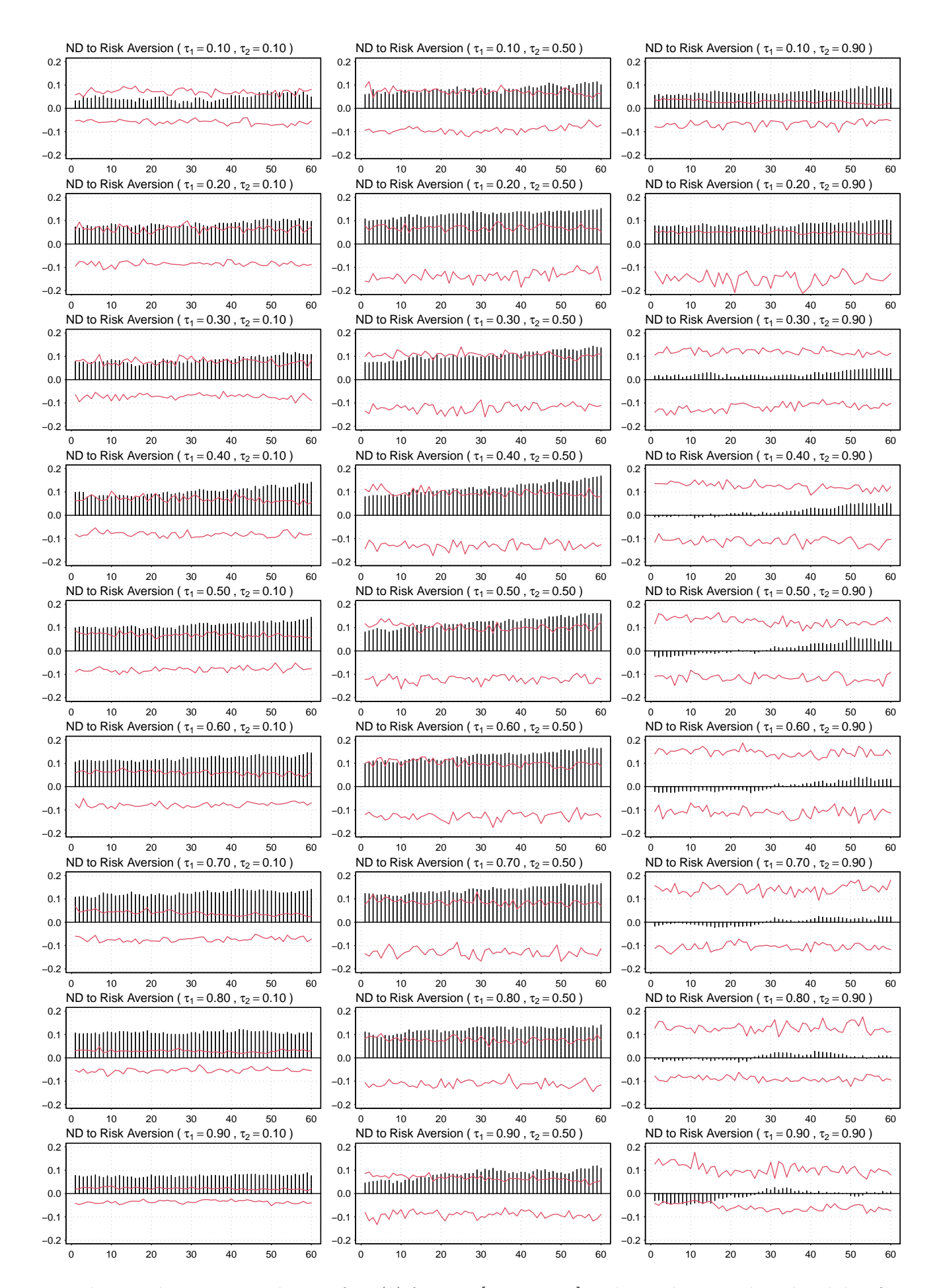


Figure 4: The sample cross-quantilogram for $\hat{\rho}(k)$ for $\tau_2 = [0.1, 0.5, 0.9]$ to detect directional predictability from ND to Risk Aversion. Bar graphs describe sample cross-quantilograms and lines are the 95% bootstrap confidence intervals centered at zero.

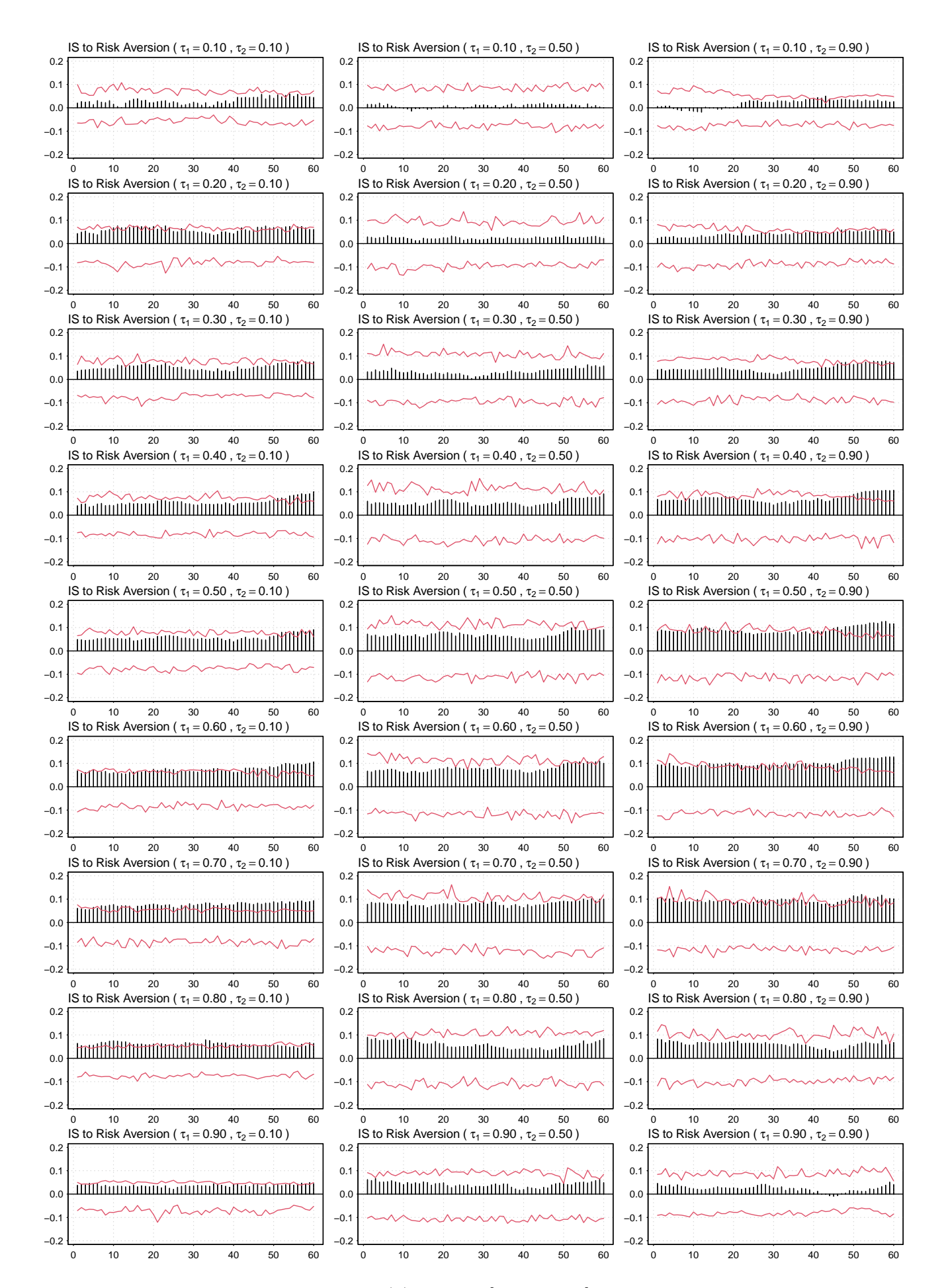


Figure 5: The sample cross-quantilogram for $\hat{\rho}(k)$ for $\tau_2 = [0.1, 0.5, 0.9]$ to detect directional predictability from IS to Risk Aversion. Bar graphs describe sample cross-quantilograms and lines are the 95% bootstrap confidence intervals centered at zero.

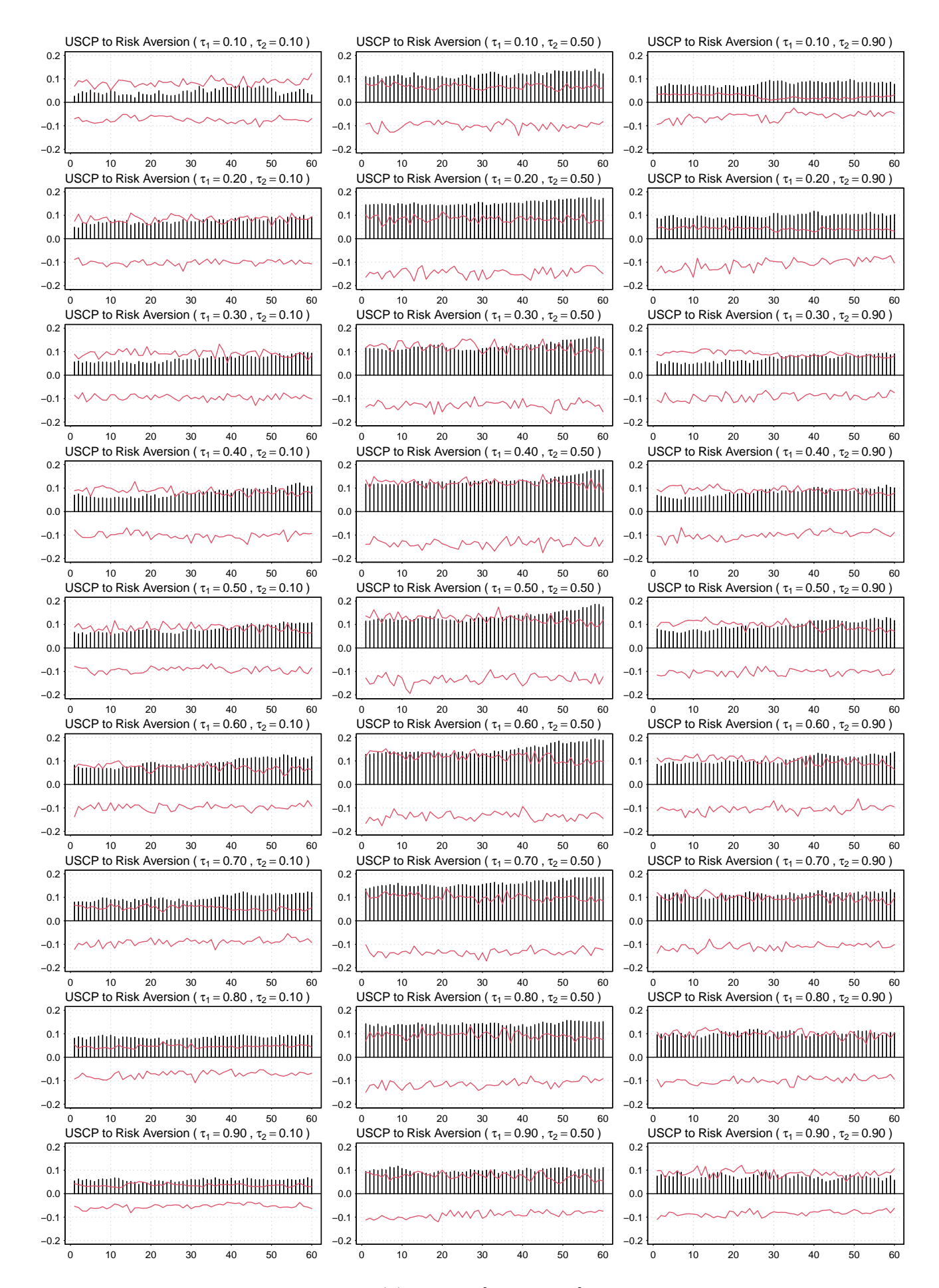


Figure 6: The sample cross-quantilogram for $\hat{\rho}(k)$ for $\tau_2 = [0.1, 0.5, 0.9]$ to detect directional predictability from USCP to Risk Aversion. Bar graphs describe sample cross-quantilograms and lines are the 95% bootstrap confidence intervals centered at zero.

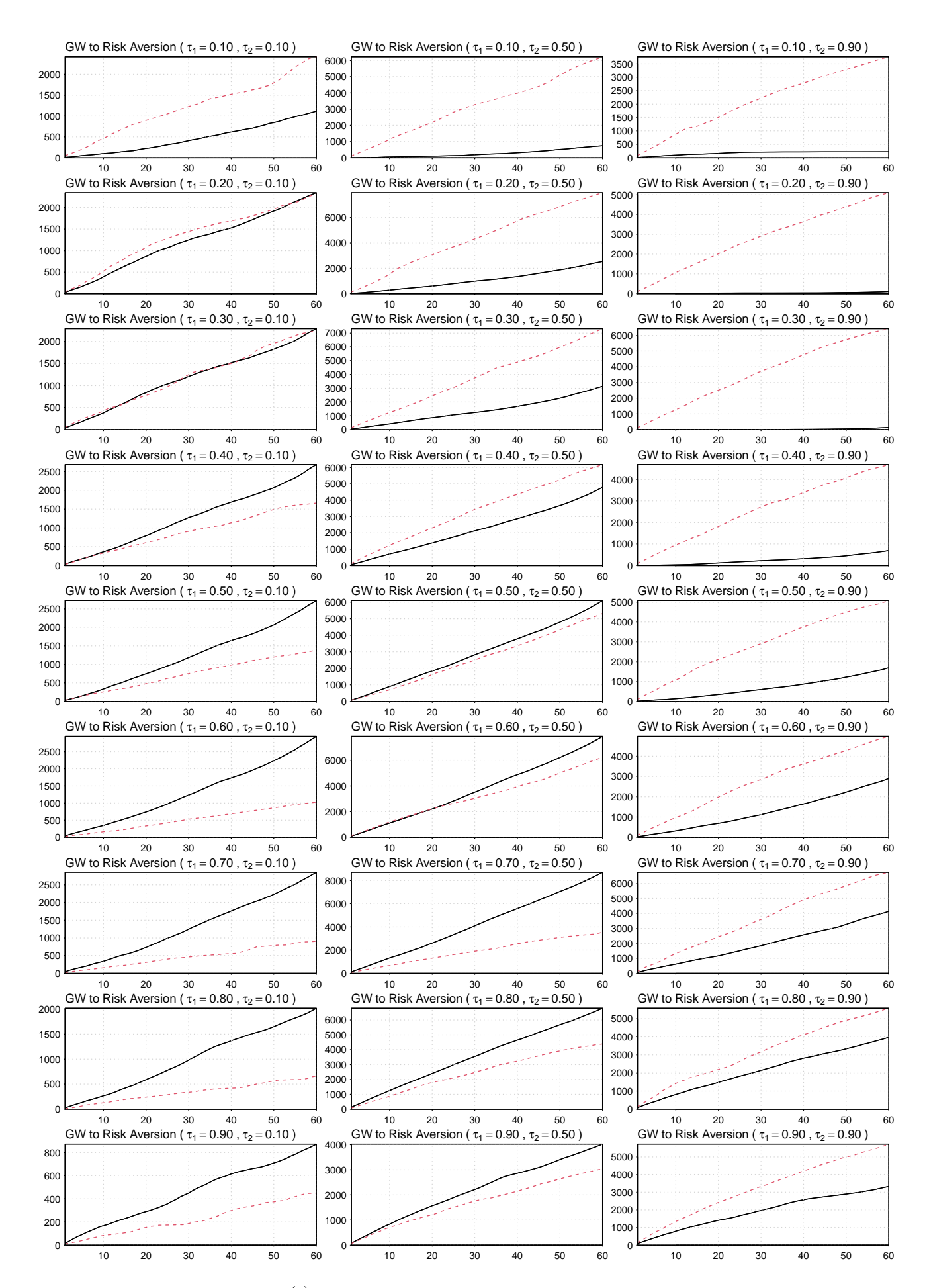


Figure 7: Box–Ljung test statistic $\hat{Q}_{\tau}^{(p)}$ for each lag p and quantile τ using $\hat{\rho}(k)$ with $\tau_2 = [0.1, 0.5, 0.9]$ from GW to Risk Aversion

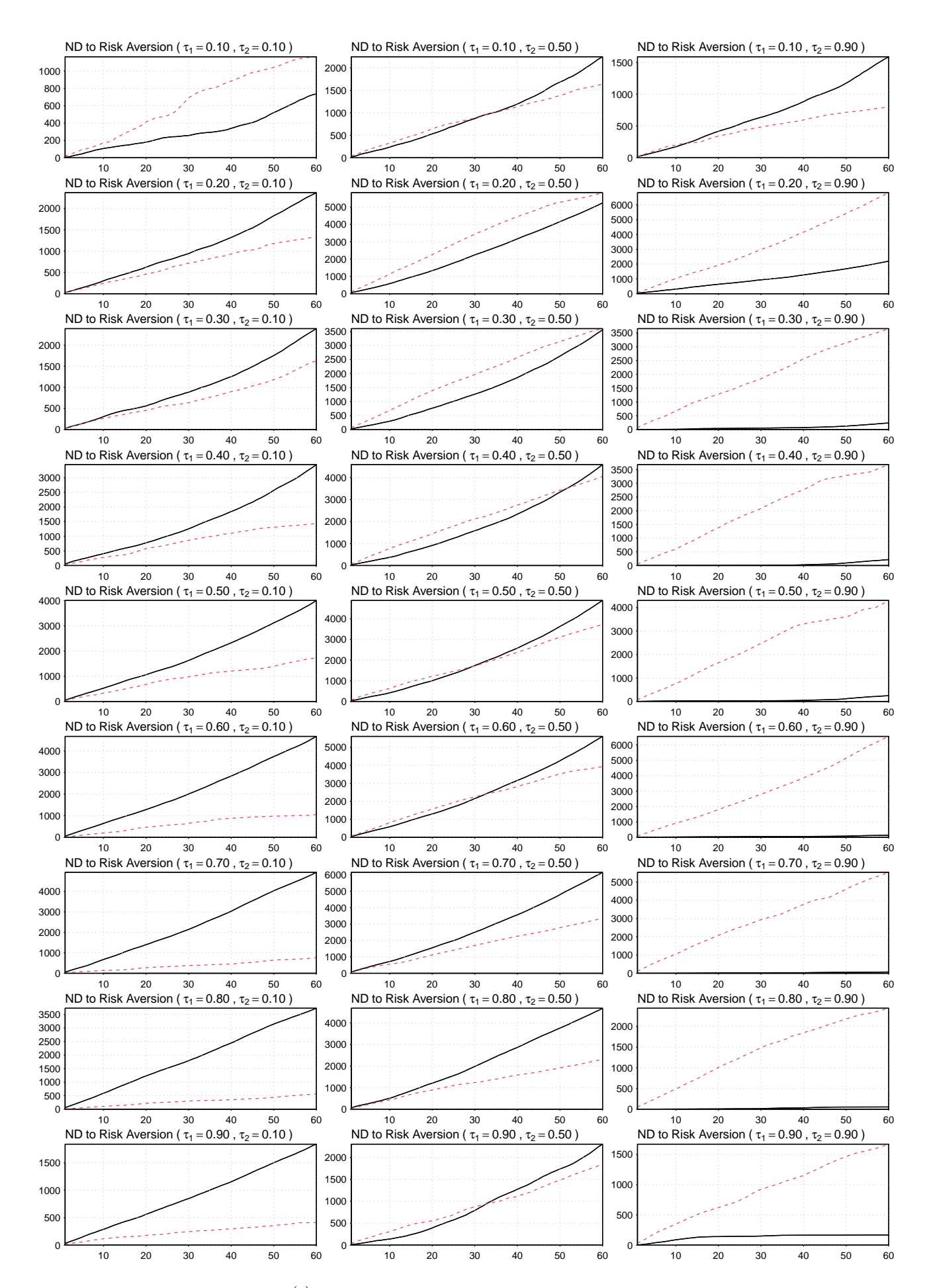


Figure 8: Box–Ljung test statistic $\hat{Q}_{\tau}^{(p)}$ for each lag p and quantile τ using $\hat{\rho}(k)$ with $\tau_2 = [0.1, 0.5, 0.9]$ from ND to Risk Aversion

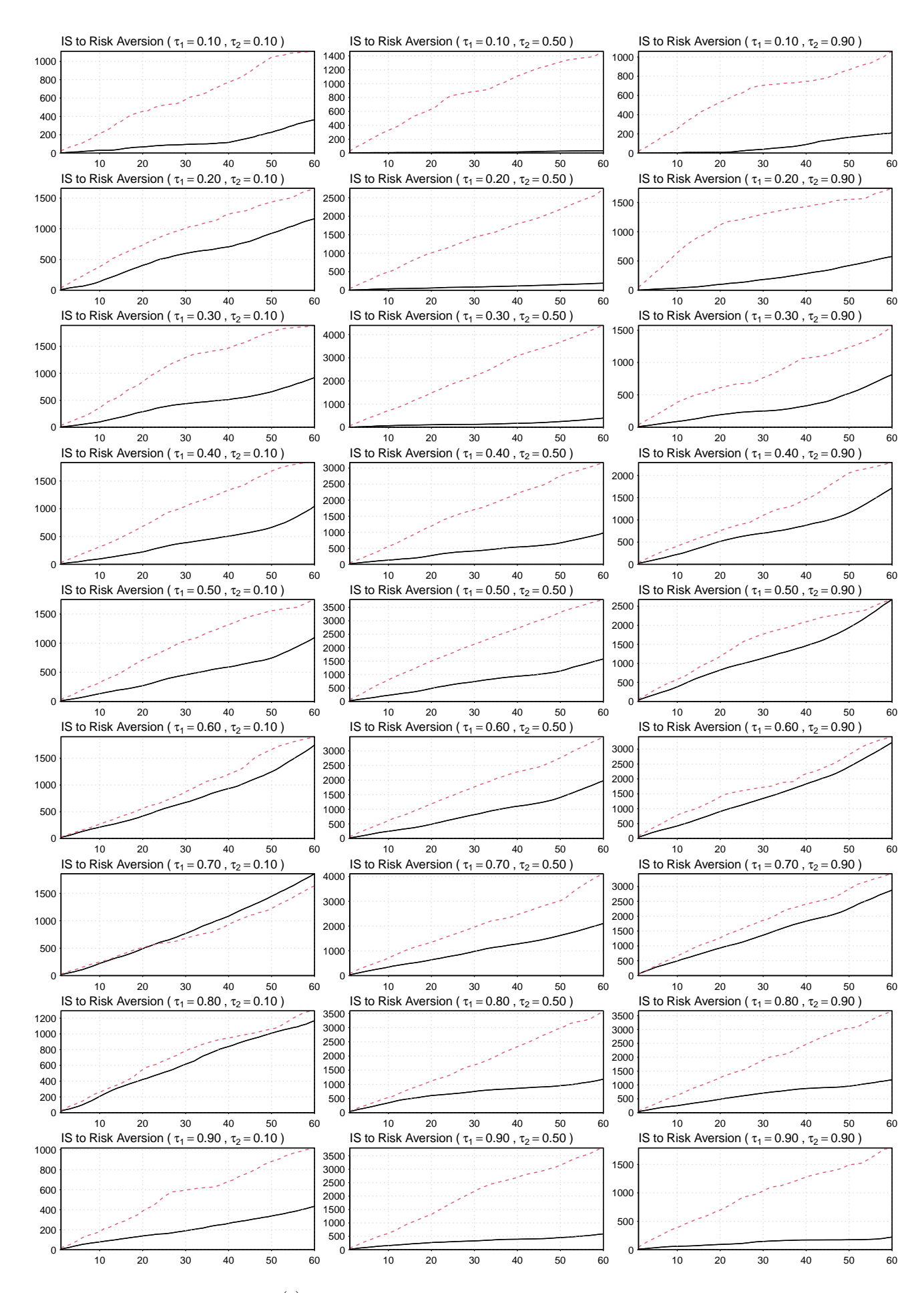


Figure 9: Box–Ljung test statistic $\hat{Q}_{\tau}^{(p)}$ for each lag p and quantile τ using $\hat{\rho}(k)$ with $\tau_2 = [0.1, 0.5, 0.9]$ from IS to Risk Aversion

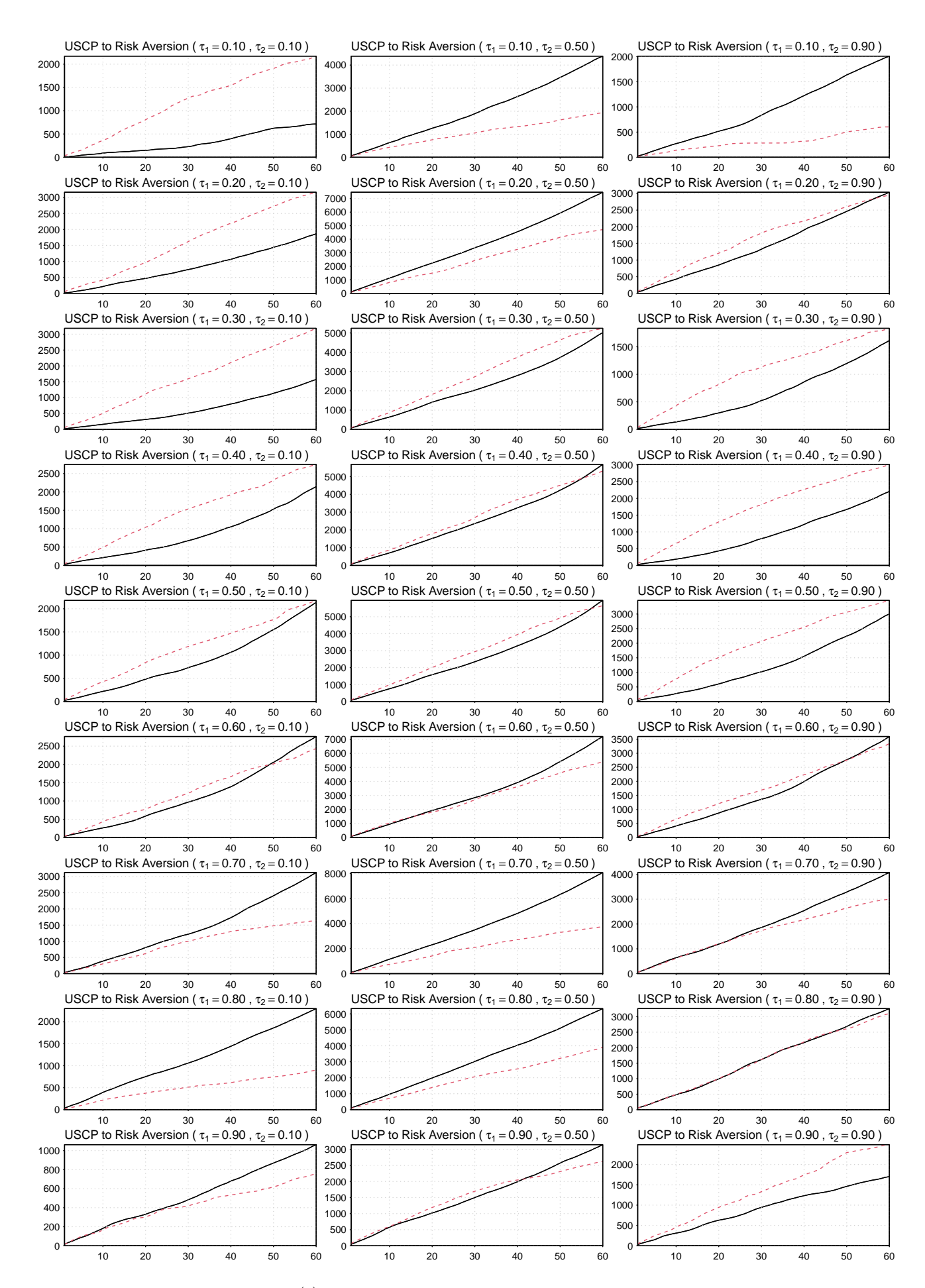


Figure 10: Box–Ljung test statistic $\hat{Q}_{\tau}^{(p)}$ for each lag p and quantile τ using $\hat{\rho}(k)$ with $\tau_2 = [0.1, 0.5, 0.9]$ from USCP to Risk Aversion

Appendix

Table A.1: Quantile causality between climate risks and alternative measures of risk aversion

	0.1	0.2	0.3	0.4	0.5	0.6	0.7	0.8	0.9
GW to RoRo	5.795***	7.074***	7.330***	6.009***	4.734***	4.590***	4.250***	4.330***	4.159***
ND to RoRo	4.699^{***}	6.128^{***}	5.840^{***}	4.986^{***}	3.214^{***}	2.740^{***}	2.990^{***}	3.711***	2.999^{***}
IS to RoRo	4.943^{***}	6.119^{***}	5.148***	3.604***	2.910^{***}	2.393**	2.386**	3.318***	2.817^{***}
USCP to RoRo	5.267^{***}	7.030***	5.992***	4.889^{***}	4.059***	3.350***	3.819***	4.171^{***}	3.930***
GW to RoRo CR	5.710***	5.932***	5.950***	5.407***	4.979***	4.685***	4.765***	5.064***	4.564***
ND to RoRo CR	5.060^{***}	5.376^{***}	4.391^{***}	4.877^{***}	5.011***	5.651^{***}	5.396^{***}	4.978^{***}	4.125^{***}
IS to RoRo CR	5.800***	6.576^{***}	5.420^{***}	6.513^{***}	5.549***	4.108***	4.724^{***}	4.620***	4.682***
USCP to RoRo CR	6.157^{***}	6.709***	6.179***	6.297^{***}	5.602***	5.290***	5.310***	5.584***	5.183***
GW to RoRo CurrGold	1.549	2.492**	2.294**	2.695***	2.796***	2.778***	2.215**	2.152**	1.629
ND to RoRo CurrGold	1.343	2.029**	2.518**	2.125**	2.471**	2.930^{***}	2.024**	1.856*	1.066
IS to RoRo CurrGold	1.098	1.538	2.047^{**}	2.130**	2.437^{**}	2.652^{***}	2.074**	1.777^{*}	1.421
USCP to RoRo CurrGold	1.455	2.439**	2.457^{**}	2.508**	3.033***	3.231***	2.643^{***}	2.171**	1.672^{*}
GW to RoRo Equity	4.486***	6.320***	6.529***	5.984***	4.995***	4.109***	3.636***	4.288***	3.946***
ND to RoRo Equity	3.755***	5.833***	5.239***	4.608***	4.225^{***}	2.985^{***}	2.975^{***}	3.025***	2.698***
IS to RoRo Equity	3.840***	5.650***	4.667^{***}	4.511^{***}	3.550***	2.897^{***}	2.925^{***}	3.236^{***}	3.081***
USCP to RoRo Equity	4.747^{***}	6.746^{***}	5.980***	4.617^{***}	4.127^{***}	3.127^{***}	2.855***	3.841***	4.316^{***}
GW to RoRo Liquidity	13.622***	18.404***	21.200***	22.497***	22.973***	22.323***	20.694***	18.530***	13.620***
ND to RoRo Liquidity	12.622***	17.150***	19.628***	20.996***	21.148***	20.850***	19.659***	17.612***	12.894***
IS to RoRo Liquidity	11.573^{***}	15.511***	17.736^{***}	19.047^{***}	19.384^{***}	19.505^{***}	18.757^{***}	16.682^{***}	12.076^{***}
USCP to RoRo Liquidity	13.519***	18.381***	21.214***	22.883***	23.133***	22.851***	21.351***	18.404***	13.603***

Note: ***, **, and * indicate significance at the 1%, 5%, and 10% levels, respectively. Null hypothesis: There is no causality between climate risks and risk aversion.

A.1 Partial Cross-Quantilogram

To account for potential confounding effects of additional variables, we extend the analysis using the partial crossquantilogram. This measure isolates the direct quantile dependence between climate risk (X_t) and Risk Aversion (Y_t) by controlling for a vector of conditioning variables \mathbf{Z}_t (see Section 2 for details about these additional variables).

Assuming \mathbf{Z}_t is an m-dimensional stationary time series with corresponding quantile-hit processes $\boldsymbol{\psi}_t^Z = (\psi_t^{Z_1}, \dots, \psi_t^{Z_m})^{\top}$, where each component is defined analogously to ψ_t^X and ψ_t^Y . The partial cross-quantilogram at lag k is based on the residuals from projecting $\psi_t^Y(\tau_1)$ and $\psi_{t-k}^X(\tau_2)$ onto ψ_t^Z :

$$\tilde{\psi}_t^Y(\tau_1) = \psi_t^Y(\tau_1) - \gamma_Y^{\mathsf{T}} \psi_t^Z, \tag{A.1}$$

$$\tilde{\psi}_{t-k}^X(\tau_2) = \psi_{t-k}^X(\tau_2) - \boldsymbol{\gamma}_X^{\mathsf{T}} \boldsymbol{\psi}_{t-k}^Z, \tag{A.2}$$

where γ_Y and γ_X are the population regression coefficients obtained by regressing the respective hit processes on ψ_t^Z . The partial cross-quantilogram is then defined as the correlation between $\tilde{\psi}_t^Y(\tau_1)$ and $\tilde{\psi}_{t-k}^X(\tau_2)$:

$$\rho_{\tau_1,\tau_2|Z}(k) = \frac{\mathbb{E}[\tilde{\psi}_t^Y(\tau_1) \cdot \tilde{\psi}_{t-k}^X(\tau_2)]}{\sqrt{\mathbb{E}[\tilde{\psi}_t^Y(\tau_1)^2] \cdot \mathbb{E}[\tilde{\psi}_{t-k}^X(\tau_2)^2]}}.$$
(A.3)

The partial cross-quantilogram enables the analysis of quantile-specific lead-lag relationships between X and Y while controlling for other variables that may confound their dependence. Estimation and inference follow similar procedures as in the unconditional case, including the use of bootstrap methods to obtain critical values.

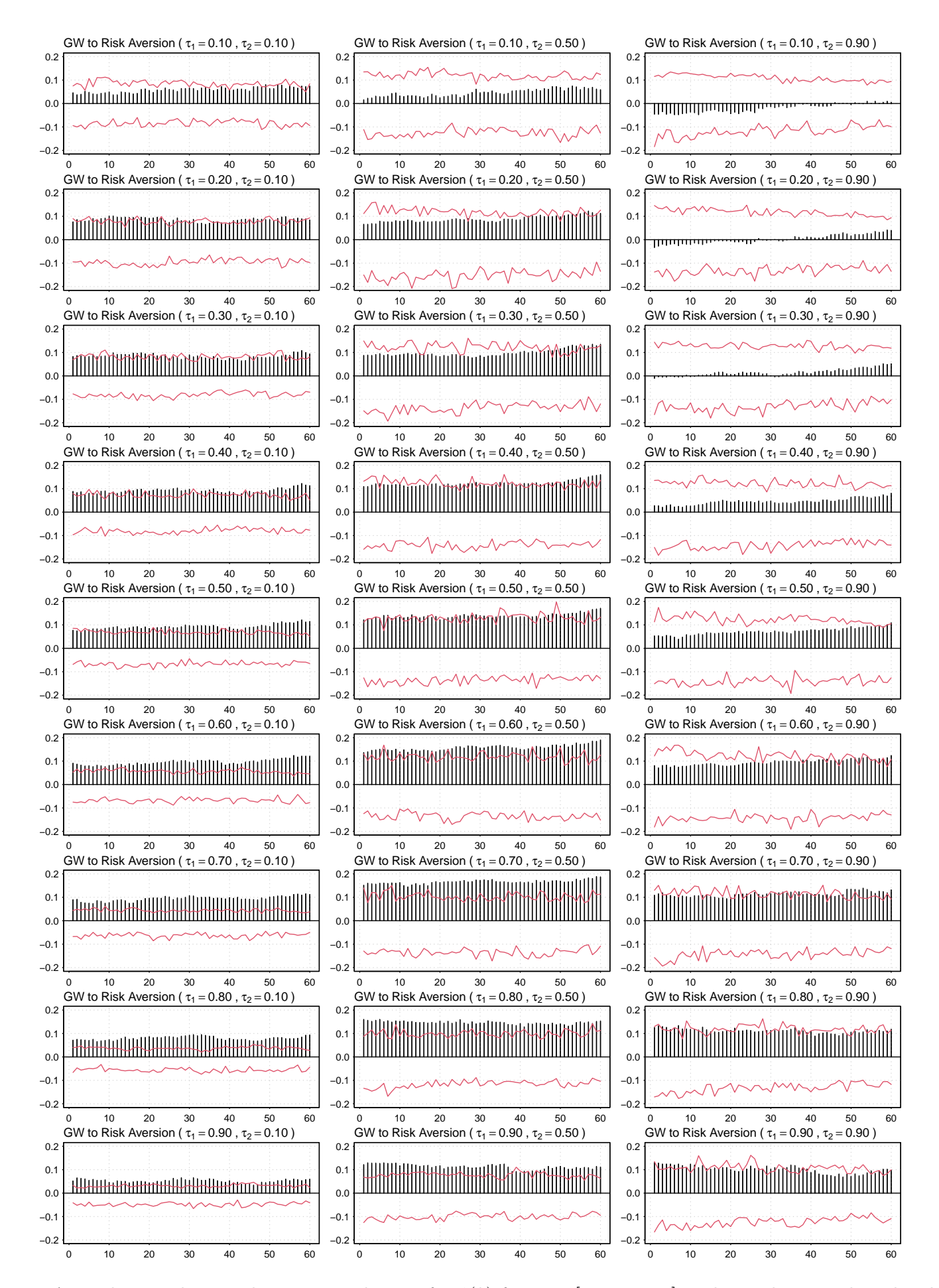


Figure A.1: The sample partial cross-quantilogram for $\hat{\rho}(k)$ for $\tau_2 = [0.1, 0.5, 0.9]$ to detect directional predictability from GW to Risk Aversion. Bar graphs describe sample partial cross-quantilograms and lines are the 95% bootstrap confidence intervals centered at zero.

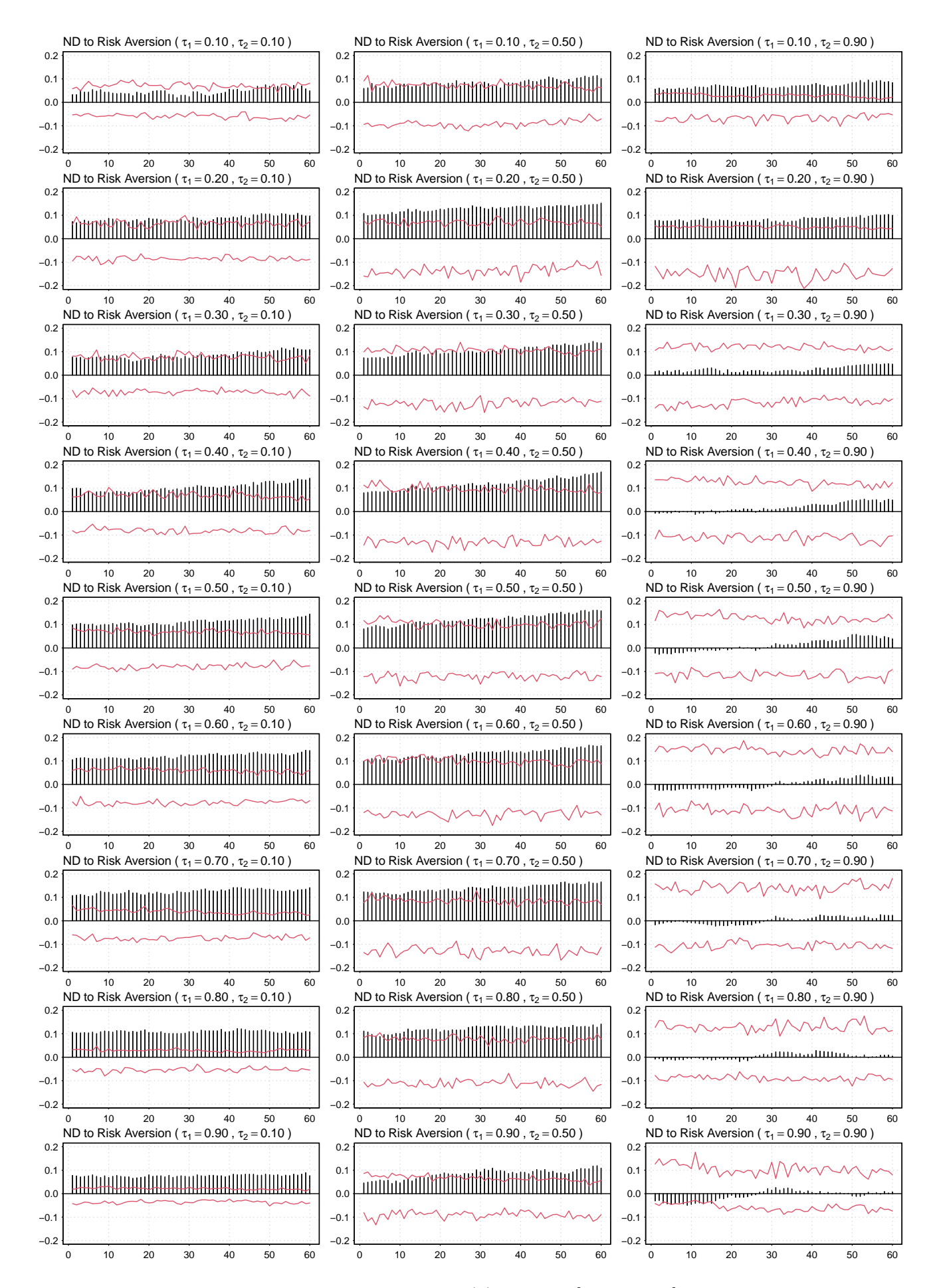


Figure A.2: The sample partial cross-quantilogram for $\hat{\rho}(k)$ for $\tau_2 = [0.1, 0.5, 0.9]$ to detect directional predictability from ND to Risk Aversion. Bar graphs describe sample partial cross-quantilograms and lines are the 95% bootstrap confidence intervals centered at zero.

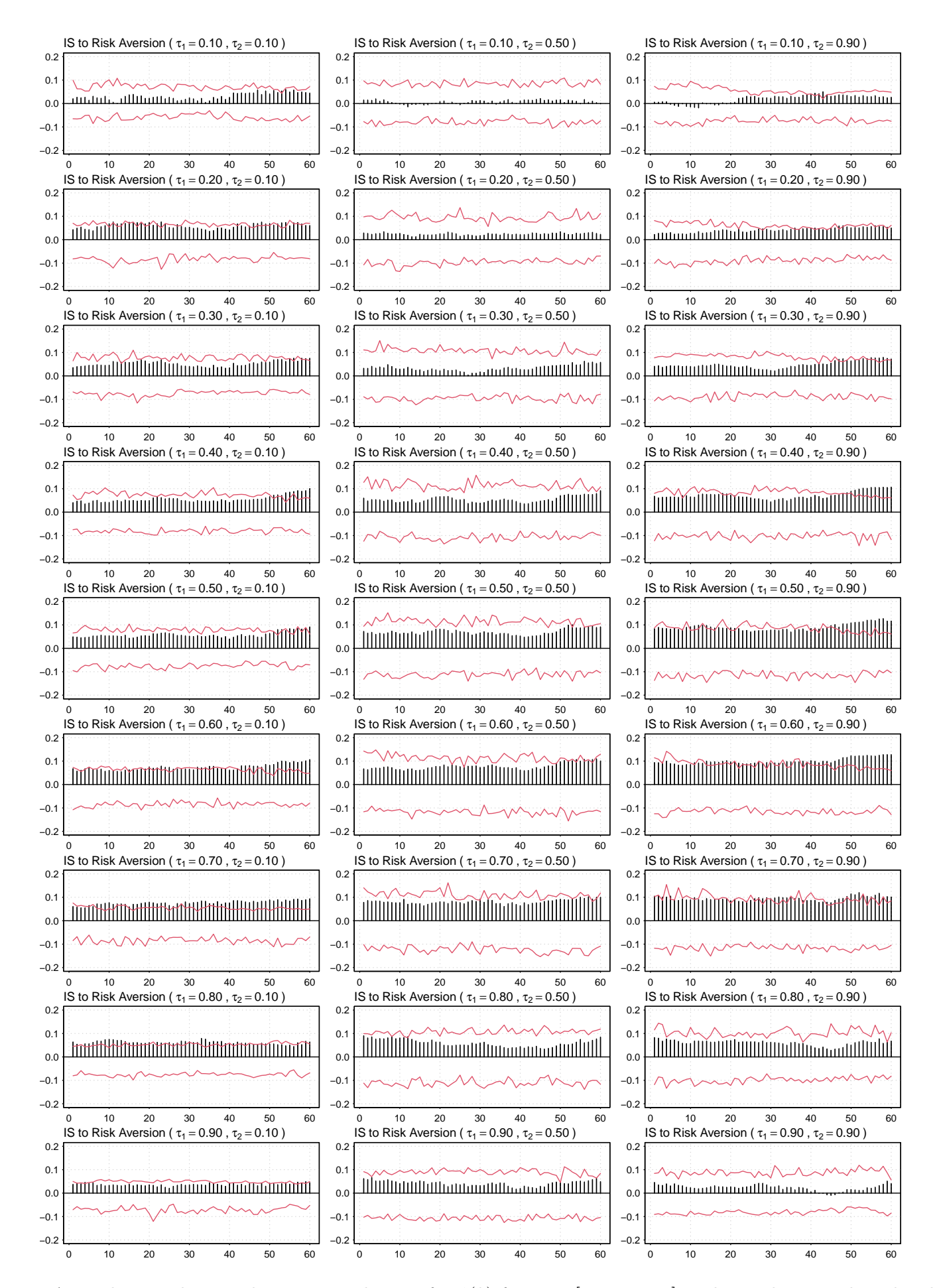


Figure A.3: The sample partial cross-quantilogram for $\hat{\rho}(k)$ for $\tau_2 = [0.1, 0.5, 0.9]$ to detect directional predictability from IS to Risk Aversion. Bar graphs describe sample partial cross-quantilograms and lines are the 95% bootstrap confidence intervals centered at zero.

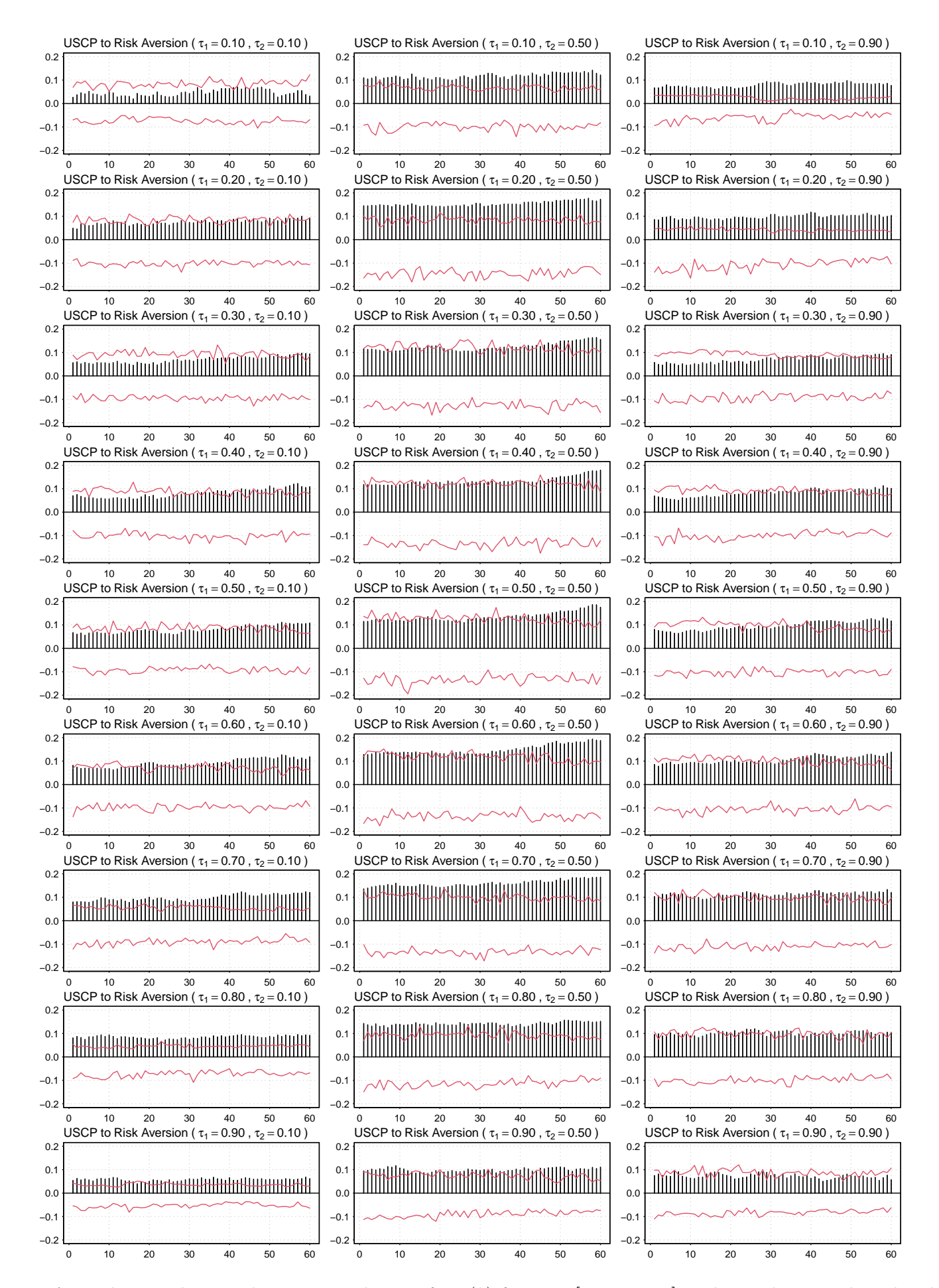


Figure A.4: The sample partial cross-quantilogram for $\hat{\rho}(k)$ for $\tau_2 = [0.1, 0.5, 0.9]$ to detect directional predictability from USCP to Risk Aversion. Bar graphs describe sample partial cross-quantilograms and lines are the 95% bootstrap confidence intervals centered at zero.